ISSN 1392–1207. MECHANIKA. 2017 Volume 23(1): 31–38

Enhancements of thermal performances of an active magnetic refrigeration device based on nanofluids

Y. Chiba*, A. Smaili, O. Sari*****

**Department of Mechanical Engineering, Faculty of Science and Technology, University of Medea, 26.000, Algeria, E-mail: Chiba.younes@univ-medea.dz*

***Ecole Nationale Polytechnique, Laboratoire de Génie Mécanique et Développement, P.B. 182,El-Harrach, Algiers, 16200, Algeria, E-mail: arezki.smaili@g.enp.edu.dz*

****University of Applied Sciences of Western Switzerland, Avenue des sports 20, 1400, Yverdon-Les-Bains, Switzerland, E-mail: osmann.sari@heig-vd.ch*

crossref http://dx.doi.org/10.5755/j01.mech.23.1.13452

Nomenclature

Standard –
A - heat transfer area, m^2; C - specific heat capacity, Jkg^{-1}K^{-1}; B - magnetic field, T; $B(X)$ - Brillouin function; COP - coefficient of performance; D_h - hydraulic diameter, M; D_B - Brownian diffusion coefficient; D_T - thermophoretic diffusion coefficient; $\dot{E}x$ - exergy, W; F - friction coefficient; g_J - Landé factor; H - Coefficient of convection heat transfer, WK^{-1}m^{-2}; J - total angular momentum quantum number; K - thermal conductivity, WK^{-1}m^{-1}; k_B - Boltzmann constant (1.38×10^{-23}), JK^{-1}; k_p - thermal conductivity of particles, WK^{-1}m^{-1}; L - length, M; MCE - magnetocaloric effect, K; M - Mass, Kg; $\dot{m}_f$ - mass-flow rate, kg s^{-1}; N_{cy} - number of cycle; N_A - modified diffusivity ratio; N_B - modified heat capacity ratio; Nu - Nusselt number; P - cooling power, W; Q - heat exchange, J; $\dot{Q}$ - heat rate, W; P - power, W; Pr - Prandtl number; R - ideal constant of gas (8.31), JK^{-1}mol^{-1}; T – temperature, °C; T_c - Curie temperature, K; T_D - Debye temperature, K; T_L - average outlet temperature, K; T_{LC} - average cold outlet temperature, K; T_{LH} - average hot outlet temperature, K; T - time, s; V - volume, m^3; $\dot{W}_p$ - pump power, W; X - spatial coordinate, m;
greek –
β_1 - non-dimensional slip coefficient; ε - porosity; φ - volume fraction of nanoparticles; γ - Sommerfeld constant, Jkg^{-1}K^2; μ - dynamic viscosity, Kg s^{-1}m^{-1}; μ_B - Bohr magneton (9.27×10^{-24}), J T^{-1}; ρ - density, kg m^{-3}; τ - time period, s;
subscripts –
bf - base fluid; C - cold; e - electronic; H - hot; L - lattice; m - magnetic; nf - nanafluid; np - nanoparticle; r - regenerator.

1. Introduction

In the past few decades, a large number of experimental and numerical studies of magnetic refrigeration devices near room temperature have been published, either in a magnetic refrigeration system or in magnetocaloric materials [1-9]. For active magnetic regenerator refrigerator device, the heat transfer plays an important role between magnetocaloric material and carrier fluid. It is strongly desirable to increase the efficiency of rate of heat exchange due to the magnetization and demagnetization of magnetocaloric material and carrier fluid. These new advanced concepts of nanofluids offer good heat transfer characteristics compared to conventional fluid.

To do this, a new concept for intensification of heat transfer was introduced by Masuda et al. 1993[10] and Choi 1995 [11] called nanofluids. It becomes possible to increase the efficiency of any machine and reduce the operating costs of magnetocaloric devices. Many researches dedicated to nanofluids are carried out in order to improve heat transfer by convection [12-13].

Different areas of application of nanofluids have been reported elsewhere by Saidur et al. 2011[14], such as:

- cooling and air conditioning systems;
- engine cooling;
- transformer cooling oil and lubrications;
- nuclear systems;
- solar energy and thermal storage;
- drilling;
- defense and space;
- biomedical applications.

The main objective of this work is to propose novel method for increasing the rate of heat exchange by convection between the carrier fluid and magnetocaloric material, a new class of fluids called nanofluids containing a small particles, such as Al_2O_3 suspended in water, have thermal properties compared with the those of the water. The results on the performance predictions obtained by using nanofluids (Al_2O_3) and water are presented and discussed.

2. Description of nanofluids

Nanofluids consisting of small particles (1-100 nm) such as (Al_2O_3, TiO_2, CuO, Cu, SiO_2,) suspended into a base fluid to improve certain thermophysical properties [13-15].

The heat transfer by using nanofluids have several advantages [14]:

- more heat transfer area between fluids and particles;
- high thermal conductivity by varying particles concentration;
- reduced pumping power as compared to conventional fluids;
- high stability.

However, nanofluids possess the following challenges:

- long term stability of nanoparticles dispersion;
- increased pressure drop and pumping power;
- higher viscosity;
- high cost of nanofluids;
- difficulties in production process.

The thermophysical properties of nanofluids; density, specific heat capacity, viscosity and thermal conductivity are dependent on the volume fraction of nanoparticles and base fluid can be defined by relationships [15]:

$$\rho_{nf} = \frac{m_{nf}}{V_{nf}} = \frac{m_{bf} + m_{np}}{V_{bf} + V_{np}} = \rho_{bf}\frac{V_{bf}}{V_{nf}} + \rho_{np}\frac{V_{np}}{V_{nf}} = \\ = (1-\varphi)\rho_{bf} + \varphi\rho_{np}, \tag{1}$$

where $\varphi = \frac{V_{np}}{V_{nf}} = \frac{m_{np}}{m_{nf}}$. (2)

$$\rho_{nf} c_{nf} = \rho_{nf}\left(\frac{Q_{nf}}{m_{nf}\Delta T}\right) = \rho_{nf}\frac{Q_{bf} + Q_{np}}{(m_{bf} + m_{np})\Delta T} = \\ = \rho_{nf}\frac{m_{bf}}{m_{nf}}c_{bf} + \rho_{nf}\frac{m_{np}}{m_{nf}}c_{np} = \rho_{nf}(1-\varphi)c_{bf} + \rho_{nf}\varphi c_{np}. \tag{3}$$

The calcul of viscosity and thermal conductivity based on semi-empirical correlations can be defined by following equations [15]:

$$\mu_{nf} = \mu_{bf}(1 + 7.74\varphi); \tag{4}$$

$$K_{nf} = k_{bf}\frac{k_p + 2k_{bf} - 2\varphi(k_{bf} - k_p)}{k_p + 2k_{bf} + \varphi(k_{bf} - k_p)}. \tag{5}$$

3. Description of magnetic refrigeration cycle

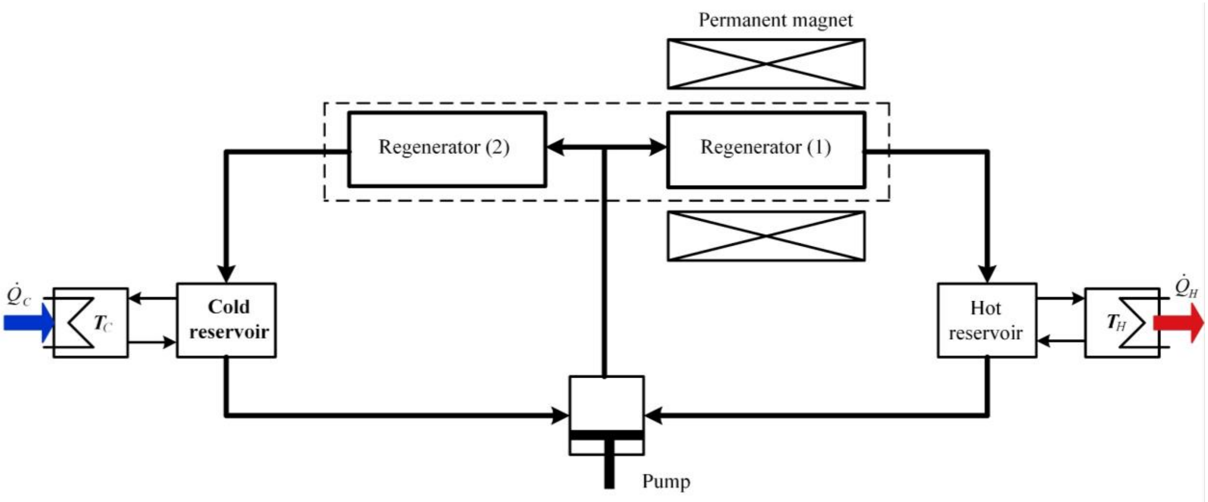

Fig. 1 Schematic diagram of the AMR cycle setup [8, 6]

Fig. 1 shows a schematic diagram of an AMR cycle developed at HE-SO, Switzerland, which is composed of (i) a two regenerators bed (i.e. magnetocaloric material which can act as refrigerant and regenerator media); (ii) a blower to force the flow throughout the regenerator at convenient velocity; (iii) a circulating heat transfer fluid (i.e. in this study nanofluid and water). The AMR cycle consists of four steps, namely, isentropic magnetization and demagnetization processe, by application and removal of a magnetic field, as well as cold and hot blows (i.e. cooling and heating the circulating fluid).

The mains steps of AMR cycle can be described in detail as follows [2, 4, 16]:

- isentropic magnetization process;
- hot blow at applied magnetic field;
- isentropic demagnetization process;
- cold blow at removed magnetic field.

4. Mathematical model

4.1. Thermodynamic approach

Based on the heat energy equation, the heat transfer through the regenerator bed of nanofluid can be written as:

$$\varepsilon\rho_{nf}c_{nf}V\frac{\partial T_{nf}}{\partial t} = hA(T_r - T_{nf}) - \dot{m}_{nf}c_{nf}\frac{\partial T_{nf}}{\partial x} + \\ + A_{nf}k_{nf}\frac{\partial^2 T_{nf}}{\partial x^2} + \left|\frac{f\dot{m}_{nf}^3}{2\rho_{nf}^2 A_{nf}^2 D_h}\right|. \tag{6}$$

The heat energy equation for magnetocaloric material can be written as:

$$(1-\varepsilon)\rho_r c_r V\frac{\partial T_r}{\partial t} = hA(T_{nf} - T_r) + A_r k_r\frac{\partial^2 T_r}{\partial x^2}. \tag{7}$$

4.2. Heat transfer

The Nusselt number characterized heat transfer by convection in the case of parallel plates between the carrier fluid and the magnetocaloric material. For base fluid (water), Nusselt number has been calculated by using correlation proposed by Ghiaasiaan, 2011[17]. For constant wall temperature (boundary condition):

$$Nu = 7.541\begin{pmatrix} 1-2.610\alpha + 4.970\alpha^2 - 5.119\alpha^3 + \\ +2.702\alpha^4 - 0.548\alpha^5 \end{pmatrix}; \quad (8)$$

$$f = 96\begin{pmatrix} 1-1.3553\alpha + 1.9467\alpha^2 - 1.7012\alpha^3 + \\ +0.9564\alpha^4 - 0.2537\alpha^5 \end{pmatrix} / Re, \quad (9)$$

where $\alpha = b/a$ with a and b are length and width respectively.

For nanofluid, Nusselt number has been calculated by using correlation proposed by Nield et al. 2014[18]:

$$Nu = 6\left(1 - \frac{2}{5}\beta^2\right) = 6\left(1 - \frac{N_A N_B}{5\varepsilon}\right), \quad (10)$$

where

$$\beta = \left(\frac{N_A N_B}{2\varepsilon}\right)^{0.5}; \quad (11)$$

$$N_A = \frac{D_T}{D_B T}; \quad (12)$$

$$N_B = \frac{\varepsilon(\rho c)_p \varphi_0^*}{(\rho c)_f}. \quad (13)$$

The coefficient D_B and D_T can be calculated by using correlation proposed by Malvandi et al. 2014[19]:

$$D_B = \frac{k_B T}{3\pi\mu_{bf} d_p}; \quad (14)$$

$$D_T = 0.26\frac{k_{bf}}{2k_{bf} + k_p}\frac{\mu_{bf}}{\rho_{bf}}\varphi. \quad (15)$$

In addition, the following correlation developed by Karimipour in 2015 can be used to determine the nanofluid Nusselt number in a microchannel as a function of:

$$\left.\begin{array}{l} 0 \le \varphi \le 0.04;\ 0.005 \le \beta_1 \le 0.05 \text{ and } 2.4 \le Pr \le 6.2; \\ Nu = 26.45\left(0.64^{\varphi}\right)\left(169.93^{-\beta}\right)\left(0.85^{Pr}\right) \end{array}\right\} \quad (16)$$

4.3. Magnetocaloric properties

The properties of magnetocaloric material has been determined by using mean field theory based on magnetism and thermodynamic. The heat specific total capacity consists of three components; namely, the magnetic heat specific capacity, electronic heat specific capacity and lattice heat specific capacity.

The total heat specific can be expressed by the equation:

$$c(B,T) = c_m(B,T) + c_l(T) + c_e(T) = \\ = T\left(\frac{\partial S_m(B,T)}{\partial T}\right) + T\left(\frac{\partial S_l(T)}{\partial T}\right) + T\left(\frac{\partial S_e(T)}{\partial T}\right), \quad (17)$$

where c_m, c_l and c_e are respectively the magnetic heat specific capacity, electronic heat specific capacity and lattice heat specific capacity.

Magnetic entropy, lattice entropy and electronic entropy is given by relation:

$$S_m(B,T) = R\begin{bmatrix} ln\, sinh\left(\frac{2J+1}{2J}\chi\right) - ln\, sinh\left(\frac{1}{2J}\chi\right) - \\ -\chi B_J(\chi) \end{bmatrix}, \quad (18)$$

where

$$\chi = \frac{g_J J \mu_B}{k_B T} + \frac{3T_C J B_J(\chi)}{T(J+1)}, \quad (19)$$

where $B_J(\chi)$ Brillouin function given by:

$$B_J(\chi) = \frac{2J+1}{2J}coth\left(\frac{2J+1}{2J}\chi\right) - \frac{1}{2J}coth\left(\frac{1}{2J}\chi\right). \quad (20)$$

Lattice entropy:

$$S_l(B,T) = R\left[-3ln\left(1 - e^{\frac{T_D}{T}}\right) + 12\left(\frac{T}{T_D}\right)^3 \int_0^{\frac{T_D}{T}} \frac{x^3}{e^x - 1}dx\right]. \quad (21)$$

Electronic entropy:

$$S_e(T) = \gamma T. \quad (22)$$

The magnetocaloric effect by using mean field theory can be calculated as function of heat specific and total entropy.

$$\Delta T_{ad} = -\int_0^B \frac{T}{c(B,T)}\left(\frac{\partial S}{\partial B}\right)dB. \quad (23)$$

4.4. Resolution method

The discretization of the energy equations of the solid and the nanofluid has been carried by using the finite differences method implicit scheme as described in the equations (Eq. (24)-(28).

The nanofluid energy equation is given by:

$$A_i T_{nfi}^{m+1} - A_{i-1} T_{nf(i-1)}^{m+1} - A_{i+1} T_{nf(i+1)}^{m+1} - C_i T_{ri}^{m+1} = T_{nfi}^m + E_i; \quad (24)$$

$$A_i = 1 + A_{i-1} + A_{i+1} + C_i = 1 + \left(\frac{k_{nf}\Delta t}{\rho_{nf} c_{nf} \Delta x^2} \mp v\frac{\Delta t}{\Delta x}\right) + \\ + \frac{k_{nf}\Delta t}{\rho_{nf} c_{nf} \Delta x^2} + \frac{hA\Delta t}{\varepsilon \rho_{nf} c_{nf} V}; \quad (25)$$

$$E_i = \frac{f\dot{m}_{nf}^3 \Delta t}{2\rho_{nf}^3 A_{nf}^3 D_h c_{nf}}. \quad (26)$$

The solid energy equation is given by:

$$B_i T_{ri}^{m+1} - B_{i-1} T_{r(i-1)}^{m+1} - B_{i+1} T_{r(i+1)}^{m+1} - D_i T_{nfi}^{m+1} = T_{ri}^m; \quad (27)$$

$$\left.\begin{aligned} B_i &= 1 + B_{i-1} + B_{i+1} + D_i = 1 + \\ &+ \frac{k_r \Delta t}{\rho_r c_r \Delta x^2} + \frac{k_r \Delta t}{\rho_r c_r \Delta x^2} + \frac{hA\Delta t}{(1-\varepsilon)\rho_r c_r V}; \\ D_i &= \frac{hA\Delta t}{(1-\varepsilon)\rho_r c_r V}. \end{aligned}\right\} \qquad (28)$$

The main steps of the resolution of the discrete equations obtained are shown in Fig. 2 as well, the system of equations obtained was resolved by using Tridiagonal Matrix Algorithm (TDMA).

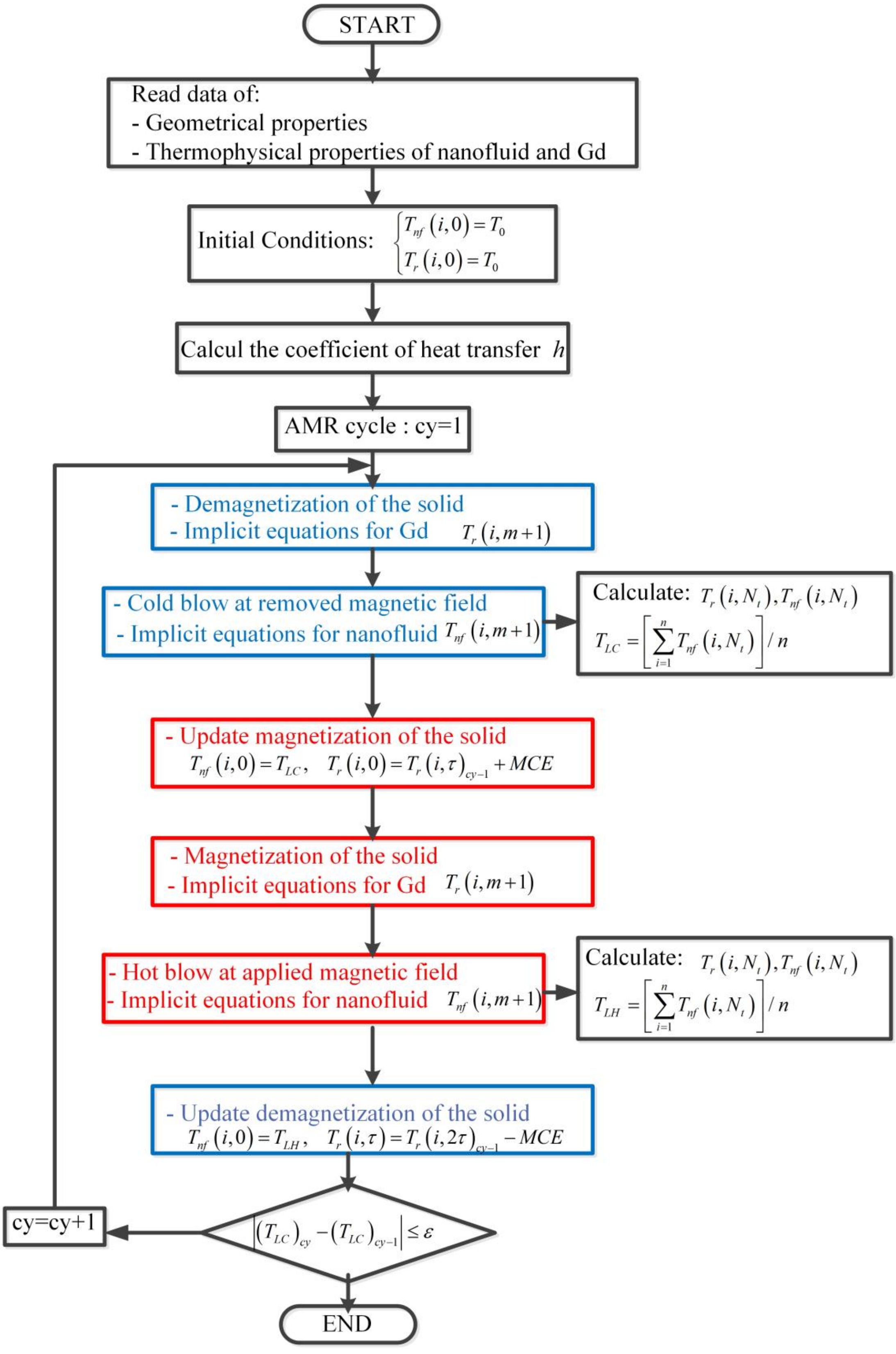

Fig. 2 Numerical algorithm AMR cycle

The average cold outlet nanofluid temperature is given by the relation:

$$T_L = \frac{1}{\tau}\int_0^{\tau} T\left(x = L, t\right) dt\,. \tag{29}$$

Once steady cyclic state is obtained, the resulting cooling capacity and coefficient of performance can be calculated as follows:

$$\dot{Q}_C = \dot{m}_{nf} c_{nf}\left(T_C - T_L\right). \tag{30}$$

The exergy and coefficient of performance of AMR cycle can be calculated as:

$$\dot{E}x = \dot{Q}_C\left(\frac{T_H}{T_C} - 1\right); \tag{31}$$

$$COP = \frac{\dot{Q}_C}{\dot{Q}_H - \dot{Q}_C + \dot{W}_P}\,. \tag{32}$$

5. Results and discussion

Table 1 shows the thermophysical properties of base fluid (water) and nanoparticles (Alumina) composed of nanofluids and used in numerical simulation of AMR device.

Table 1
Thermophysical properties of base fluid and nanoparticles

	ρ, Kg/m^3	c_p, J/kg K	k, J/s m K	μ, Kg/m s
Water (H_2O)	998.2	4182	0.597	$9.93.10^{-4}$
Alumina (Al_2O_3)	3970	765	36	-

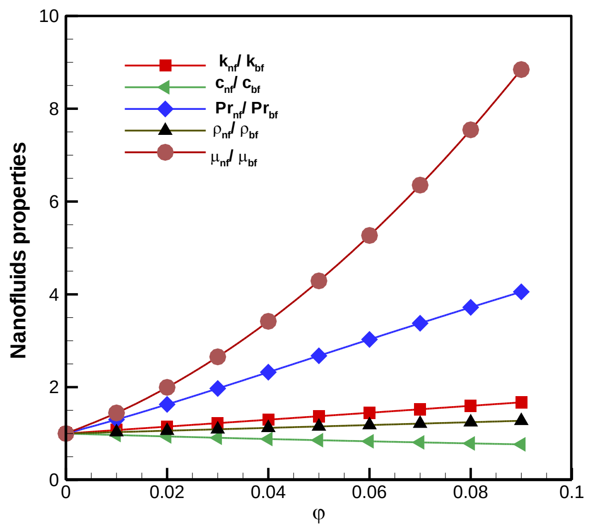

Fig. 3 Impact of nanoparticle volume fraction on thermophysical properties of nanofluids

Fig. 3 shows variation of ration of thermophysical properties (thermal conductivity, specific heat, density and Prandtl number) of nanofluids as function of nanoparticle volume fraction. Fig. 3 illustrates clearly the positive impact of the increase of the volume of the particles on number of Prandtl and the thermal conductivity and negative impact on the viscosity and the specific heat.

The results presented in Fig. 4, show the variation of magnetocaloric effect under magnetic field of 2*T* and specific heat capacity at magnetic field of 0*T* and 2*T* as function of the temperature for magnetocaloric material Gadolinium by using molecular field theory approach. These properties have been injected in numerical model to compute the physical parameters of active magnetic refrigerator.

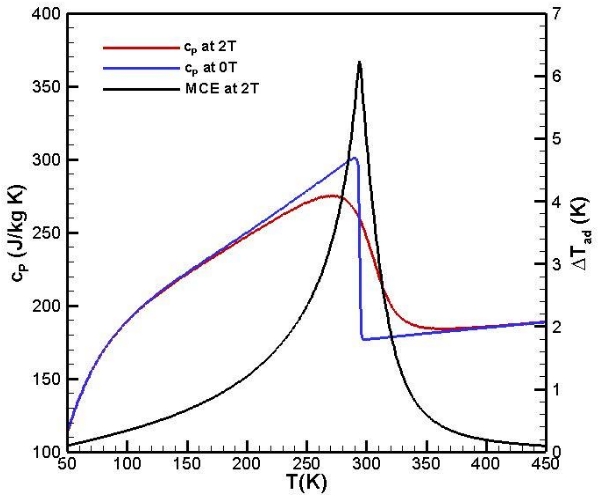

Fig. 4 Variation of adiabatic temperature and specific heat as function of temperature.

Fig. 5 shows impact of frequency on the evolutions of the average cold outlet temperature of nanofluid without load under magnetic field of 2*T* as function of cycle number. As it can be seen, all the curves exhibit sharp decreasing trends with number of cycle, then an asymptotic behaviour towards the steady state. More the frequency value is higher more is slower the convergence towards the steady state.

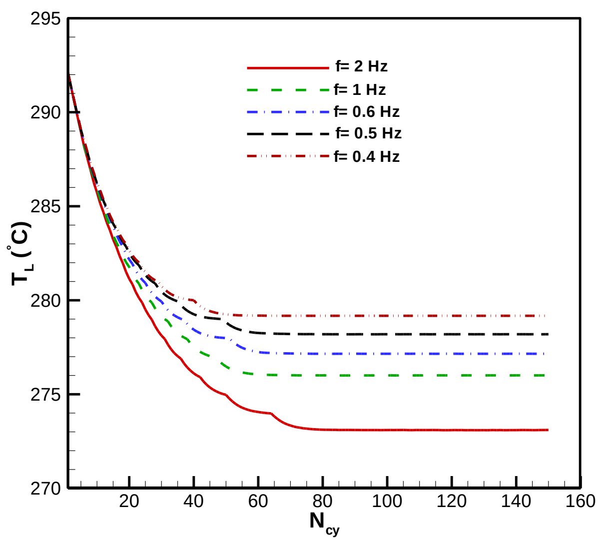

Fig. 5 Variation of average temperature cold reservoir as function of cycle number at different values of frequency without load under magnetic field of 2*T*

Fig. 6 and Fig. 7 show respectively evolution of exergy as a function of span temperature and as a function of cold temperature under magnetic field of 2*T* and operating parameters; namely, mass flow rate of 0.15 kg/s and temperature of hot exchanger of 21°C. As it can be seen, differences up to 15% have been noted between nanofluid and water.

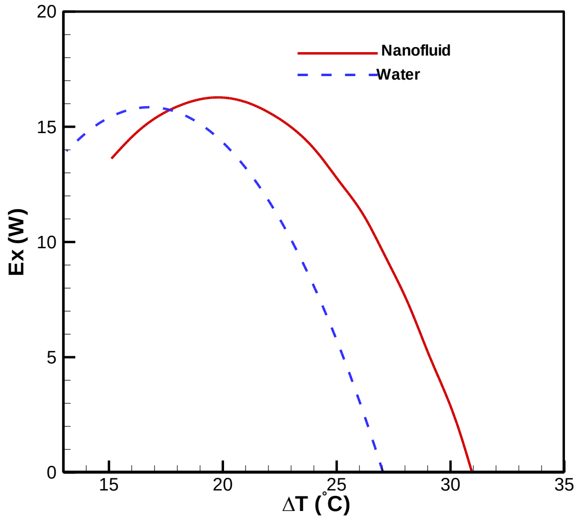

Fig. 6 Evolution of exergy as function of temperature span

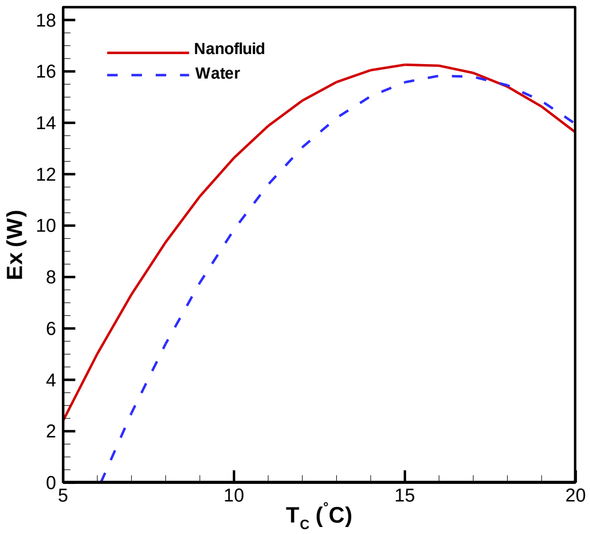

Fig. 7 Evolution of exergy as function of cold temperature

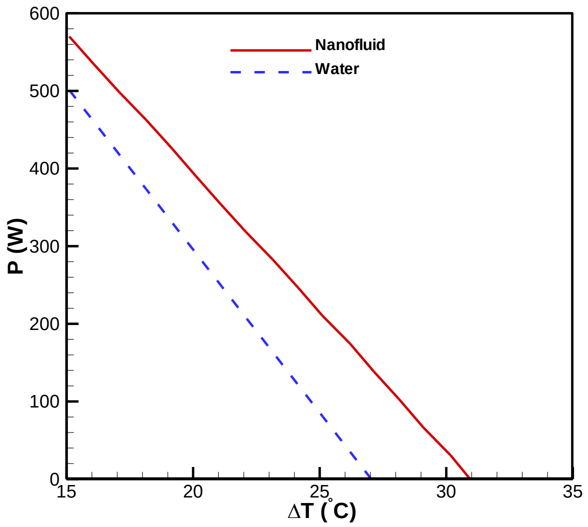

Fig. 8 Evolution of cooling power as function of temperature span

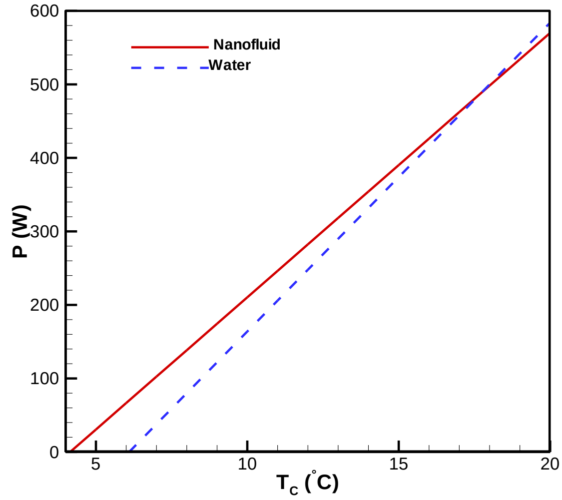

Fig. 9 Evolution of cooling power as function of cold temperature

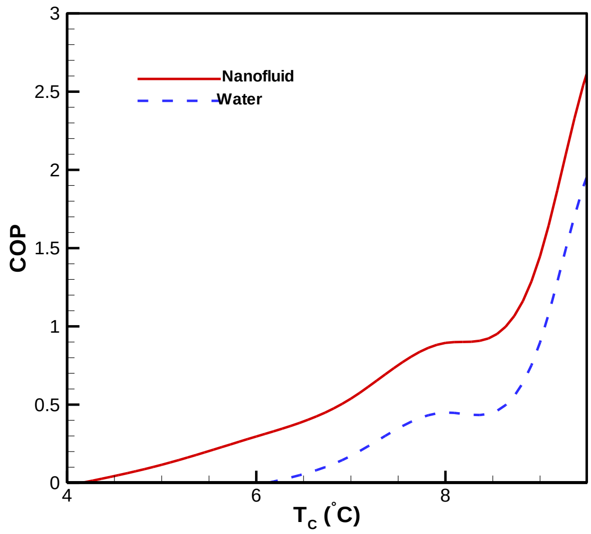

Fig. 10 Evolution of coefficient of performance as function of cold temperature

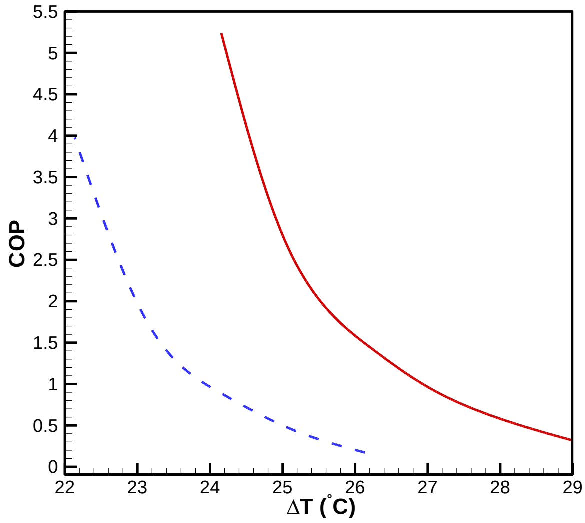

Fig. 11 Evolution of coefficient of performance as function of span temperature

Fig. 8 and Fig. 9 show respectively evolution of cooling power as function of temperature span and cold temperature under magnetic field of 2*T* and operating parameters; namely, mass flow rate of 0.15 kg/s and temperature of hot exchanger of 21°C. As it can be seen, differences up to 15% have been noted between nanofluid and water. Fig. 10 and Fig. 11 show respectively evolution of coefficient of performance as function of temperature span and cold temperature under magnetic field of 2*T* and operating parameters; namely, mass flow rate of 0.15 kg/s and temperature of hot exchanger of 21°C. As it can be seen, differences up to 15% have been noted between nanofluid and water.

6. Conclusion

In this paper, a numerical study on a magnetic refrigeration device operating near room temperature has been carried out. The obtained results confirm that nanofluid offers higher heat performance than water with differences about to 15% have been noted.

The potential of nanofluids is promising and can be considered for the future fluids for the enhancement and intensification of heat transfer on multi-domain. The proposed numerical model and the obtained results enable us to clarify the opportunity and utility of using and applying nanofluids in magnetic refrigeration devices. Finally, future works will be focus on experimental study to validate the numerical model and the results obtained of this model will be used again by comparing with other type of nanofluids.

References

1. **Yu, B.; Liu, M.; Egolf, P.W.; Kitanovski, A**. 2010. A review of magnetic refrigerator and heat pump prototypes built before the year 2010, International Journal of Refrigeration 33: 1 029-1060. http://dx.doi.org/10.1016/j.ijrefrig.2010.04.002.
2. **Romero Gómez, J.; Ferreiro Garcia, R.; Carbia Carril, J.; Romero Gómez, M**. 2013. A review of room temperature linear reciprocating magnetic refrigerators, Renewable and Sustainable Energy Reviews 21: 1-12. http://dx.doi.org/10.1016/j.rser.2012.12.018.
3. **Smaïli, A.; Chahine, R.** 1998. Thermodynamic investigations of optimum active magnetic regenerators, Cryogenics 38: 247-252. http://dx.doi.org/10.1016/S0011-2275(97)00140-9.
4. **Chiba, Y.**; **Smaili, A.**; **Mahmed, C.**; **Balli, M.**; **Sari, O**. 2014. Thermal investigations of an experimental active magnetic regenerative refrigerator operating near room temperature, International Journal of Refrigeration 37: 36-42. http://dx.doi.org/10.1016/j.ijrefrig.2013.09.038.
5. **Bouchekara, H.; Kedous-Lebouc, A.; Dupuis, C.; Allab, F**. 2008. Prediction and optimisation of geometrical properties of the refrigerant bed in an AMRR cycle, International Journal of Refrigeration 31: 1224-1230. http://dx.doi.org/10.1016/j.ijrefrig.2008.02.007.
6. **Tishin, A.; Y. Spichkin** .2003. The magnetocaloric effect and its applications. Institute of Physics Publishing. http://dx.doi.org/10.1887/0750309229.
7. **Roudaut, J.; Kedous-Lebouc, A.; Yonnet, J.-P.; Muller, C**. 2011. Numerical analysis of an active magnetic regenerator, International Journal of Refrigeration 34: 1797-1804. http://dx.doi.org/10.1016/j.ijrefrig.2011.07.012.
8. **GschneidnerJr., K.A.; Pecharsky, V.K**. 2008. Thirty years of near room temperature magnetic cooling: Where we are today and future prospects, International Journal of Refrigeration 31: 945-961. http://dx.doi.org/10.1016/j.ijrefrig.2008.01.004.
9. **Egolf, P.W.; Vuarnoz, D.; Gravier, L.; Courret, G.** 2012. The thermodynamics of devices with solid layered-bed magnetocaloric refrigerants, International Journal of Refrigeration 35: 1506-1517. http://dx.doi.org/10.1016/j.ijrefrig.2012.05.008.
10. **Masuda, H.; Ebata, A.; Teramae, K.; Hishinuma, N.** 1993. Alteration of thermal conductivity and viscosity of liquid by dispersing ultrafine particles (dispersion of γ-Al_2O_3, SiO_2, and TiO_2 ultra-fine particles), Netsu Bussei 4(4): 227-233. http://dx.doi.org/10.2963/jjtp.7.227.
11. **Choi, S**. 1995. Enhancing thermal conductivity of fluids with nanoparticles, ASME Fluids Eng Div (Publ) FED 231: 99-105.
12. **Ozerinc¸ S.; Kakac, S.; Yazıcıoglu. A. G.** 2010. Enhanced thermal conductivity of nanofluids: a state-of-the-art review, Microfluid Nanofluid 8: 145-170. http://dx.doi.org/10.1007/s10404-009-0524-4.
13. **Sarkar, J.; Ghosh, P.; Adil, A.** 2015. A review on hybrid nanofluids: Recent research, development and applications, Renewable and Sustainable Energy Reviews 43: 164-177. http://dx.doi.org/10.1016/j.rser.2014.11.023.
14. **Saidur, R.; Leong, K.Y.; Mohammad, H.A**. 2011. A review on applications and challenges of nanofluids, Renewable and Sustainable Energy Reviews 15: 1646-1668. http://dx.doi.org/10.1016/j.rser.2010.11.035.
15. **Bianco, V.; Manca, O.; Nardini, S.; Vafai, K**. 2015. Heat Transfer Enhancement with Nanofluids, CRC Press, Taylor & Francis Group, 481 p.
16. **Kitanovski, A.; Tusek, J.; Tomc, U.; Plaznik, U.; Ozbolt, M.; Poredos, A.** 2015. Magnetocaloric Energy Conversion: From Theory to Applications, Springer International Publishing, 456 p. http://dx.doi.org/10.1007/978-3-319-08741-2.
17. **Ghiaasiaan, M**. 2011. Convective heat and Mass Transfer, Cambridge University Press, New York, USA, 550 p. http://dx.doi.org/10.1017/CBO9780511800603.
18. **Nield, D.A.; Kuznetsov, A.V.** 2014. Forced convection in a parallel-plate channel occupied by a nanofluid or a porous medium saturated by a nanofluid, International Journal of Heat and Mass Transfer 70: 430-433. http://dx.doi.org/10.1016/j.ijheatmasstransfer.2014.04.051.
19. **Malvandi, A.; Ganji, D**. 2014. Effects of nanoparticle migration on force convection of alumina/water nanofluid in a cooled parallel-plate channel, Advanced Powder Technology 25: 1369-1375. http://dx.doi.org/10.1016/j.apt.2014.03.017.

Y. Chiba, A. Smaili, O. Sari

ENHANCEMENTS OF THERMAL PERFORMANCES OF AN ACTIVE MAGNETIC REFRIGERATION DEVICE BASED ON NANOFLUIDS

S u m m a r y

In this work, an analytical study on the active magnetic regeneration cycle operating near room temperature using nanofluid as carrier fluid, in order to enhance the heat transfer in regenerator bed after magnetization and demagnetization process. For this purpose, a nanofluid based on Al_2O_3 has been proposed. A numerical simulation of 1D model based on the transient energy equations is used to describe the heat transfer between the magnetocaloric material and the carrier fluid in the regenerator bed. The obtained results are presented, discussed and compared with base fluid.

Keywords: Nanofluid, Al_2O_3, Gadolinium, Active magnetic regenerator, Thermal analysis.

Received October 21, 2015
Accepted February 06, 2017